Carbon sources and sinks of North America as affected by major drought events during the past 30 years

Zelalem A.Mekonnen[a]Robert F.Grant[a]ChristopherSchwalm[b]

Abstract

The North American (NA) terrestrial biosphere has been a long-term carbon sink but impacts of climate extremes such as drought on ecosystem carbon exchange remain largely uncertain. Here, changes in biospheric carbon fluxes with recent climate change and impacts of the major droughts of the past 30 years on continental carbon cycle across NA were studied using a comprehensive mathematical process model, *ecosys*. In test of these model responses at continental scale, the spatial anomalies in modeled leaf area indices, fully prognostic in the model, from long-term (1980–2010) means during major drought events in 1988 and 2002 agreed well with those in AVHRR NDVI (R^2 = 0.84 in 1988, 0.71 in 2002). Net ecosystem productivity (NEP) modeled across NA declined by 92% (0.50 Pg C yr^{-1}) and 90% (0.49 Pg C yr^{-1}) from the long-term mean (+0.54 Pg C yr^{-1}), in 1988 and 2002 respectively. These significant drops in NEP offset 28% of the carbon gains modeled over the last three decades. Although the long-term average modeled terrestrial carbon sink was estimated to offset ~30% of the fossil fuel emissions of NA, only 0.03% and 3.2% were offset in 1988 and 2002 leaving almost all fossil fuel emissions to the atmosphere. These major drought events controlled much of the continental-scale interannual variability and mainly occurred in parts of the Great Plains, southwest US and northern Mexico. Although warming in northern ecosystems caused increasing carbon sinks to be modeled as a result of greater gross primary productivity with longer growing seasons, elsewhere in the continent frequent drought events of the past 30 years reduced carbon uptake and hence net carbon sinks of the NA.

Keywords: North America drought, North America carbon cycle, Climate change, Ecosystem modeling, Carbon source and sink

1. Introduction

Current estimates of CO_2 exchange across North America (NA) have shown that on an annual time scale the continental biosphere has been long-term carbon sink (Huntzinger et al., 2012, King et al., 2007, Peters et al., 2007) that has partly offset fossil fuel emissions. King et al. (2007) estimated that the NA biosphere was a sink for 30% of the continental fossil fuel emissions of 1.85 Pg C yr^{-1} in 2003. However, there have been spatial and temporal variability in carbon sources and sinks attributed to changes in climate (Baldocchi et al., 2001, Goulden et al., 1996), particularly during disturbances (Lindroth et al., 2009) and extreme climate events such as drought (Jentsch et al., 2007, Zhao and Running, 2010, Zscheischler et al., 2014).

Studies have shown that areas affected by drought have increased in the last four decades (Dai et al., 2004). The frequency and intensity of droughts have also increased (Huntington, 2006) and are projected to increase under future climate change scenarios (IPCC, 2013). Climate change such as warming and changes in precipitation over recent decades have been observed in most regions of NA and the past decade has included the warmest years within the instrumental record of global surface temperature (IPCC, 2007, Shaver et al., 2000). Warming could increase specific humidity by increasing evaporation, and consequently increase precipitation and intensify the water cycle (Held and Soden, 2000, Huntington, 2006). Intensifying the water cycle may increase the intensity and frequency of floods and droughts (Huntington, 2006). As drought is a disturbance of the water cycle (van der Molen et al., 2011), it can have direct effects on ecosystem carbon cycling and may have carry-over effects (Reichstein et al., 2013) in subsequent years.

Drought directly affects net ecosystem productivity (NEP) through its effects on component fluxes (NEP = gross primary productivity (GPP) − ecosystem respiration (R_e)) (Gaumont-Guay et al., 2006), and contributes to most of the interannual variability in carbon exchange (Ciais et al., 2005, Jentsch et al., 2007, Pereira et al., 2007). The extent of drought at continental scale can be assessed using indices (e.g. normalized difference vegetation index(NDVI), enhanced vegetation index (EVI)) derived from remote sensing products such as Moderate Resolution Imaging Spectroradiometer (MODIS), Advanced Very High Resolution Radiometer (AVHRR) and Landsat (Caccamo et al., 2011, Karnieli et al., 2010, Wan et al., 2004). However, these large scale satellite products have some limitations: their accuracy varies with land cover and soil types (Gu et al., 2008); they may be unable to detect short-term water stress in areas with deep-rooted trees that may sustain water availability(Caccamo et al., 2011); they do not estimate changes in NEP and they lack predictive capability under future climate. Drought can also be assessed using a top-down atmospheric inversion approach with atmospheric transport models (Knorr and Heimann, 1995, Peters et al., 2007) that estimate net ecosystem exchange (NEE) but do not provide estimates of the component fluxes. Although drought indices such as Palmer Drought Severity Index (PDSI) (Alley, 1984) and Standard Precipitation Index (SPI) (Hayes et al., 1999) can be used to examine drought status at continental scale, the actual magnitude of carbon fluxes cannot be assessed using these indices. Earlier efforts to model regional drought effects included different approaches that use statistical nonlinear regression models (Reichstein et al., 2003) and diagnostic models such as radiation-use efficiency models (Jamieson et al., 1995).

In a more comprehensive approach, here we used a mathematical process model, *ecosys*(Grant, 2001, Grant, 2014) to simulate the effects of major droughts of the past 30 years on carbon fluxes. This approach is based on the fundamental theory of how water moves through the soil-plant-

atmosphere and how this movement affects GPP and R_e, explicitly formulated in the model (Grant et al., 2012, Grant et al., 2006a, Grant and Flanagan, 2007). This water transfer scheme of the model has been used to examine the underlying biophysical processes during drought and the subsequent effects of soil water deficit on NEP and component fluxes. Soil water deficit during drought reduces GPP in the model by reducing soil water potential (Ψ_s) and increasing soil hydraulic resistance which lowers canopy water potential (ψ_c) and stomatal conductance (g_c), forcing declines in CO_2 diffusion and carboxylation (Grant et al., 1999). Concurrently, a reduction in the supply of labile carbon, due to a decline in GPP, reduces autotrophic respiration (R_a) and less soil moisture availability for microbial activity reduces heterotrophic respiration (R_h) resulting a decline in R_e ($R_a + R_h$) (van der Molen et al., 2011), although this decline is usually smaller than that in GPP.

The coupled schemes for soil-plant-atmosphere water transfer and CO_2 exchange of the model have been rigorously tested at site scale against eddy covariance (EC) measured CO_2 and energy fluxes over a wide range of climates across different biomes: seasonally dry grassland in a Mediterranean climate zone under variable rainy seasons from 2001 to 2008 ($0.7 < R^2 < 0.9$) (Grant et al., 2012); semi-arid grassland in Lethbridge, Alberta under the 2001–2003 drought vs. good rainfall ($0.74 < R^2 < 0.83$) (Grant and Flanagan, 2007, Li et al., 2004), cropland in Nebraska with irrigated vs. rainfed maize-soybean rotation in 2002–2003 ($R^2 > 0.8$) (Grant et al., 2007b); boreal aspen forest in Saskatchewan under the 2001–2003 drought ($R^2 > 0.72$) (Grant et al., 2006a), and in several temperate and boreal deciduous and coniferous forests under variable weather, for 9 EC sites from 1998 to 2006 ($0.87 < R^2 < 0.63$, except for the old Jack pine (SOJP) site with $R^2 = 0.57$ in 2004) (Grant et al., 2009, Grant et al., 2006b).

While these modeled impacts of drought on ecosystem productivity were captured when tested at the various EC sites, the model responses of continental carbon cycle to major drought events during recent decades has not been assessed prior to this study. Although inverse and inventory studies indicate substantial reductions in net carbon uptake by terrestrial ecosystems during droughts in NA, these droughts are highly regional and so therefore are these reductions. In this study, we propose to examine the sensitivity of NA net carbon uptake to the major droughts of the past 30 years. The impact of these major droughts on the carbon uptake vs. ecosystem respiration and the subsequent effect on annual and long-term carbon budget of the continent has been assessed.

2. Methods

2.1. Model description

A detailed description of inputs, parameters and algorithms used in *ecosys* can be found in Grant, 2001, Grant, 2014 and Grant et al., 2011b, Grant et al., 2012. However, the general descriptions of the algorithms and

parameters that are most relevant to modeling the impacts of soil water stress during drought on ecosystem productivity are given below and details of the equations used are given in Appendices A–C of the Supplement.

2.2. Effects of water stress on CO_2 fixation (GPP)

The soil-plant-atmosphere water transfer scheme is implemented by calculating ψ_c from a two-stage convergence solution. The first stage is the convergence to canopy temperature (T_c) at which the first-order closure of the canopy energy balance (net radiation R_n (Eq. B1a), latent heat flux LE (Eqs. B1b, c)), sensible heat flux H (Eq. B1d), and change in heat storage G is achieved (Grant et al., 2011a). After convergence for T_c, canopy transpiration(E_c) is coupled with total water uptake from all rooted soil layers U (Grant et al., 1999), through a convergence solution for Ψ_c at which E_c equals U + change in plant water storage(Eq. B14). The U from the soil to the canopy is determined by the potential difference between ψ_c and ψ_s across hydraulic resistances in soil Ω_s (Eq. B9) and roots Ω_r (Eqs. B10–B12) in each rooted soil layer (Eq. B6) (Grant et al., 2007a). The E_c from the canopy to the atmosphere is governed by r_c which rises from a minimum value, $r_{cmin,}$ aggregated by leaf surface area from r_{lmin} (Eq. B2a) at zero Ψ_c through an exponential function of canopy turgorpotential Ψt (Eq. B2b) calculated from Ψc and osmotic water potential $\Psi\pi$ (Eq. B4). After convergence for T_c and $\psi_{c,}$ CO_2 fixation V_c is calculated under ambient ψ_c and r_c from stomatal and non-stomatal effects of canopy water status (Grant and Flanagan, 2007), through the convergence solution for intercellular (C_i) and canopy (C_c) gaseous CO_2concentration at which rates of diffusion and CO_2 fixation are equal as described in Grant and Flanagan (2007b). Soil drying during drought raises Ω_s and lowers Ψ_s, thereby lowering ψ_c required to keep U in equilibrium with E_c, inducing rises in canopy (r_c) and leaf (r_l) resistances (Grant et al., 1999) and hence a decline in CO_2 diffusion and carboxylation as demonstrated in Grant and Flanagan (2007). A decline in carboxylation slows input to plant nonstructural carbon pools that drive R_a and thereby growth of biomass and leaf area index(LAI), which are thus also slowed by lower ψ_c.

2.2.1. Effect of water stress on heterotrophic respiration (R_h)

Decomposition rate of each organic matter-microbe complex (coarse woody litter, fine non-woody litter, manure, particulate organic matter and humus) represented in *ecosys* is determined by the active biomass M of heterotrophic microbial populations (Eq. A1) and the substrate concentration (Eq. A3) (Grant et al., 2006a). Decomposition rate is controlled by $T_s$through an Arrhenius function (Eq. A6) and by θ through its effect on aqueous microbial concentrations [M] (Eq. A3). T_s and θ are calculated from surface energy and water exchanges coupled with soil heat and water transfers through atmosphere-canopy-snow-surface residue-soil profiles (Grant et al., 2012). Decomposition generates dissolved organic carbon (DOC) that drives microbial growth through R_h. Rate of R_h is also controlled by microbial N and P concentrations, DOC, T_s, O_2, ψ_s. Total R_h drives CO_2 emission from soil

through diffusion and volatilization in aqueous and gaseous phases (Grant et al., 2012). Lower θ from soil drying during drought raises [*M*], slowing organic matter decomposition through a competitive inhibition effect on specific activity of *M*, hence lowering DOC and reducing R_h and subsequent growth of *M* that further slows decomposition.

2.3. Model drivers

Gridded datasets for climate, soil, land use/land cover dynamics, CO_2 concentration, nitrogen deposition and disturbance across North America were used as inputs to drive *ecosys* (Table 1) as described in Mekonnen et al. (2016a). The climate dataset used in this study was the North American Regional Reanalysis (NARR) produced at the National Oceanic and Land Administration (NOAA) National Center for Environmental Prediction (NCEP) Global Reanalysis (Mesinger et al., 2004, Wei et al., 2014). We used a NARR dataset which was made available through the Multi-Scale Synthesis and Terrestrial Model Inter-comparison Project (MsTMIP) (Wei et al., 2014). This dataset extended from 1979 to 2010 with a temporal resolution of 3-h, and was interpolated linearly to 1-h for use in *ecosys*. The NARR climate variables used to drive *ecosys* were air temperature at 2m, total precipitation at surface, downward shortwave radiation flux at surface, relative humidity and wind speed.

Table 1. Model drivers and temporal resolution used to drive *ecosys* (Mekonnen et al., 2016a).

Model Drivers	**Temporal period**	**Temporal resolution**	**Data source**
Climate	1979–2010	3-h	NARR[a]
Soil	One time	One time	UNASM[b](SSURGO (US) + SLC v3.2 (CA) + HWSD v1.1 (MX))
CO_2	1800–2010	Monthly	Enhanced GlobalView[a]
Nitrogen deposition	1800–2010	Yearly	Enhanced Dentener[a]
Land use change	1800–2010	Yearly	Hurtt’s harmonized with SYNMAP[a]

*All gridded model inputs had 0.25 × 0.25 spatial resolutions.

a. MsTMIP model drivers (Wei et al., 2014).

b. Unified North America Soil Map (Liu et al., 2013).

The Unified North America Soil Map (UNASM) which was a reanalysis product of MsTMIP for North America that was prepared using three different soil databases (Liu et al., 2013) was used as a model input. The soil attributes used were layer depth, clay/sand fraction, pH, total organic carbon, cation exchange capacity and bulk density. Land use/land cover was modeled from a dataset for the years 1800–2010 developed by merging Hurtt historical land cover classification (Hurtt et al., 2006) and 2000/2003 SYNMAP land cover classification (Jung et al., 2006) products (Wei et al., 2014). The atmospheric CO_2 concentration used in the model was created from GLOBEVIEW-CO_2 as described in Wei et al. (2014). Annual nitrogen deposition used in the model was derived from Dentener's global atmospheric nitrogen deposition maps in the years of 1860 and 1993 (Dentener, 2006). The annual variation of nitrogen deposition rate from 1890 to 1990 was controlled by EDGAR-HYDE 1.3 (van Aardenne et al., 2001) nitrogen emission data (Wei et al., 2014). Nitrogen deposition was assumed to increase linearly over the remaining period up to the present (1990–2010).

Fire was introduced as external forcing in the model simulation. Four different data sources for Canada, US and Mexico were harmonized to create a continuous historical fire disturbance dataset as described in Mekonnen et al. (2016a). The datasets used were the Canadian wildfire information system, US Land Fire Product Global Fire Emission Database (GFED), and NACP Forest Age Maps (Pan et al., 2011). These different products of fire disturbance were not consistent in spatial and temporal resolutions and were in different data models (point and polygon vectors, and raster). Therefore, the products were all geo-rectified, interpolated and re-gridded to a 0.25° × 0.25° spatial resolution to make it consistent with the projection and spatial resolution of the other model drivers used in this study. The carbon transformations and emissions during fire disturbance and the effect on NEP is explicitly modeled in *ecosys* (Grant et al., 2010, Wang et al., 2011).

2.4. Simulation design

Model runs for each grid cell (0.25° × 0.25°) across NA were prepared with time-varying drivers for a simulation period of 1800–2010. To represent historical weather, NARR data from 1979 to 1993 were randomly distributed to form a 100 year sequence that cycled through 1800–1978. This enabled the model to attain a steady state prior to 1979. Then the real time NARR data were used for the rest of the period (1979–2010) to simulate real time ecosystem productivity as described in Mekonnen et al. (2016a) and MsTMIP protocol (Huntzinger et al., 2013). The model was initialized with attributes from the UNASM soil dataset, and run under dynamic land use/land cover changes, atmospheric CO_2concentrations, nitrogen deposition and disturbances (Table 1).

2.5. Model testing

2.5.1. Site scale

Fluxes measured at EC towers offer the best constrained test of modeled drought effects, although this can only be conducted at a site scale. Modeled annual CO_2 exchange aggregated from hourly values in pixels corresponding to the locations of 13 EC flux towers were compared with EC-derived values in selected contrasting years (drought vs. non-drought) with available EC data (Barr et al., 2013). To demonstrate how water stress affects modeled CO_2 and energy exchanges during drought at a fine scale temporal resolution, hourly time scale, we compared fluxes of CO_2, latent heat (LE) and sensible heat (H) modeled vs. measured at a mixed grass prairie EC flux tower site in Lethbridge (CA-Let) during a drought (2001) vs. non-drought (2002) year. Modeled fluxes were extracted from the pixel of the NA run in which the CA-Let EC tower was located. Differences in NARR vs. measured annual precipitation of 194 vs. 216 mm during 2001 and 492 vs. 582 mm during 2002 allowed the comparison of effects of water stress on modeled vs. measured carbon exchange at CA-Let. Furthermore the preceding year 2000 was also dry with lower NARR vs. measured precipitation of 207 vs. 275 mm resulting in carry-over effects to the drought in 2001, providing an opportunity to test modeled responses of carbon and energy exchanges to severe water stress at this site.

2.5.2. Continental scale

Remote sensing products such as MODIS GPP and AVHRR NDVI can be used to test modeled drought effects. Thus, modeled GPP was compared with MODIS GPP and GPP derived and upscaled from network of EC observations (Jung et al., 2011) for 2002 (drought year) vs. 2005 (non-drought year). We could not compare the GPP for the drought year 1988 as the MODIS product was not available for that year. Changes in spatial patterns of LAI from long-term averages modeled during drought years 1988 and 2002 were compared with those in NDVI from AVHRR. LAI in *ecosys* is fully prognostic and so represents drought effects on leaf expansion and primary productivity. The declines in modeled LAI could be correlated to a similar reduction in NDVI through its effect on the fraction of absorbed photosynthetically active radiation (fAPAR). Satellite fAPAR products are derived from surface reflectances that indicate canopy energy absorption capacity (Myneni et al., 2002) and are thus affected by LAI, while NDVI values are strongly correlated to fAPAR in which increasing NDVI values indicate increasing vegetation density (Box et al., 1989, Carlson and Ripley, 1997). Geographically weighted regression (GWR) was used to test the relationships between changes in the spatial patterns of the modeled LAI and AVHRR NDVI. Modeled NEP was also compared with other estimates such as atmospheric inversion modeling from CarbonTracker.

2.6. Analysis of data and model outputs

Drought indices derived from long-term precipitation data can be used to test the extent of precipitation deviations from the long-term normal prior to using the dataset to model the effects of drought on carbon fluxes. Thus,

standardized precipitation index (SPI) was used to assess drought conditions, independent of the model, based on the long-term (1979–2010) precipitation data from NARR. SPI was computed to test the drought status at monthly time scale for the growing season (June, July and August) during the drought years of 1988 and 2002. SPI measured drought status based on a probability index calculated from monthly precipitation aggregated from NARR data for a particular time scale (moving average for 3, 6, 12 etc. months), by fitting to a Gamma function to determine relationship between probability and precipitation and then transforming to a normal distribution (McKee et al., 1993). Mean values were set to zero and negative values indicate dry periods (< −2, extremely dry; −1 to −1.99, moderate to severely dry; 0.99 to −0.99, near normal) whereas positive values represented wet periods (> 2, extremely wet; 1–1.99, moderate to very wet).

To examine the effects of drought on continental scale land-atmosphere carbon exchange, hourly modeled GPP, R_e and NEP for the years 1980 − 2010 were aggregated to annual totals for each grid cell to create continuous gridded data across NA for each year of the study. Annual outputs of modeled mid-August LAI were extracted from each grid cell across NA. To analyze the long-term (1980–2010) temporal trends of carbon fluxes for NA the spatially averaged values were computed considering area of grid cells as a weighting factor. The spatial pattern of reductions in modeled annual GPP and mid-August LAI, and mid-August NDVI from AHVRR caused by droughts in 1988 and 2002 were computed by subtracting gridded long-term values from those for the drought years. Spatial patterns of interannual variability in NARR precipitation, modeled mid-August LAI and NDVI, as affected by drought, were assessed using relative standard deviation (RSD = (SD/absolute value of long-term mean) × 100).

3. Results

3.1. Model testing

3.1.1. Site scale

Reductions in modeled annual GPP, and NEP during selected drought vs. non-drought years were corroborated with similar reductions in EC-derived values across different EC sites ($R^2$for modeled vs. EC-derived GPP (0.88) and EC-derived NEP (0.87)) (Fig. 1(a1, a2)). Similar comparison of modeled GPP vs. GPP extracted from a gridded product upscaled from network of EC observations (Jung et al., 2011) have shown good agreement (R^2 = 0.69) (Fig. 1a3). Much of the modeled and EC-derived carbon sinks during non-drought years were offset by carbon sources during the drought years (Table 2), shown by the large reductions in NEP as a result of droughts such as in 2002/03 compared to 2005 for most of the EC sites (Fig. 1 (b1, b2, b3)), indicating widespread declines in productivity in 2002 through much of central and western NA.

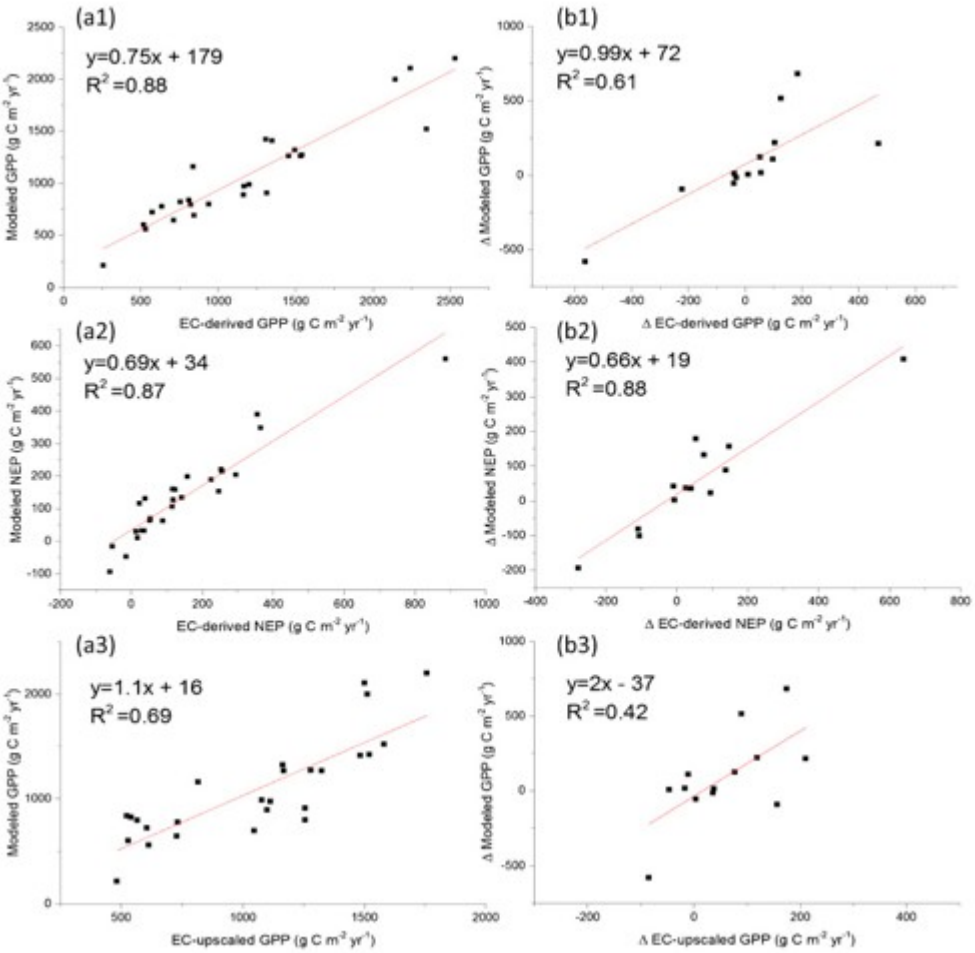

Fig. 1. Correlation between (a1, b1) modeled vs. EC-derived GPP (a2, b2) modeled vs. EC-derived NEP (a3, b3) modeled vs. EC-upscaled (Jung et al., 2011) GPP for (a1, a2, a3)combined years of drought (2002) and selected non-drought years (b1, b2, b3) changes (non-drought - drought year) across 13 EC flux tower sites in Table 2.

Table 2. Modeled vs. EC-derived annual C budgets for selected contrasting years (drought vs. non-drought) for 13 EC flux tower sites. Modeled values were taken from the grid cells in the continental run corresponding to the locations of the EC tower sites.

EC site	Ecosystem	Lat	Lon	Year	C balance[a] − modeled				C balance[a] − derived from EC measurements				
					GPP	Re	NEP	%Δ[b]	GPP	Re	NEP	%Δ[b]	Source[f]
CA-NS1	Boreal black spruce	55.8	−98.4	2002[d]	600	616	−16	−114	520	572	−53	−330	(Goulden et al., 2006)
				2005[e]	722	606	116		573	550	23		
CA-Ojp	Old Jack Pine	53.9	−104.6	2002[d]	558	605	−47	−136	530	544	−15	−138	(Kljun et al., 2006)
				2005[e]	777	646	131		634	594	39		
US-NR1	Subalpine forest	40	−105.5	2003[d]	821	818	29	−54	754	741	13	−75	(Monson et al., 2005)
				2006[e]	837	773	64		809	756	53		
US-Ton	Savanna woodland	38.4	−120.9	2003[e]	891	757	134	−75	1163	1021	142	−74	(Ma et al., 2007)
				2005[d]	798	765	33		940	904	36		

EC site	Ecosystem	Lat	Lon	Year	C balance[a] − modeled				C balance[a] − derived from EC measurements				
					GPP	Re	NEP	%Δ[b]	GPP	Re	NEP	%Δ[b]	Source[f]
US-Var	Grassland	38.4	−120.9	2001/02[cd]	694	788	−94	−251	844	904	−60	−168	(Ma et al., 2007)
				2004/05[ce]	907	845	62		1313	1225	88		
CA-Let	Mixed grass prairie	49.7	−112.9	2002[e]	793	589	204	−95	822	527	295	−94	(Flanagan and Adkinson, 2011)
				2001[d]	212	202	10		258	240	18		
US-Ha1	Deciduous forest	42.5	−72.2	2002[d]	1265	1076	189	77	1533	1308	225	94	(Urbanski et al., 2007)
				2003[e]	1271	1164	107		1543	1426	116		
US-UMB	Arboreal forest	45.6	−84.7	2002[d]	988	830	158	−1	1200	1075	124	6	(Gough et al., 2008)
				2003[e]	973	813	160		1168	1051	117		
US-	Evergre	45	−68.	2002[d]	13	11	19	−1	14	13	15	−3	(Richard

EC site	Ecosystem	Lat	Lon	Year	C balance[a] – modeled				C balance[a] – derived from EC measurements				
					GPP	Re	NEP	%Δ[b]	GPP	Re	NEP	%Δ[b]	Source[f]
Ho1	Eden forests	45.2	−72.1	2003[e]	2064	1044	220	0	1455	1202	253	8	(Hollinger et al., 2009)
CA-Obs	Mature Black Spruce	53.9	−105.1	2002[d]	643	611	32	−53	712	683	29	−46	(Krishnan et al., 2009)
				2005[e]	1158	1089	69		838	784	54		
US-DK3	Loblolly pine forest	35.9	−79.1	2002[d]	1519	1366	153	−73	2346	2099	247	−72	(Oren et al., 2006)
				2005[e]	2200	1640	560		2530	1644	886		
US-MMS	Deciduous forests	39.3	−86.4	2002[d]	1409	1061	348	−11	1347	982	365	2.5	(Schmid et al., 2000)
				2005[e]	1421	1031	390		1309	953	356		
CA-CA1	Douglas-fir	49.8	−125.3	2002[d]	1998	1871	127	−40	2145	2027	118	−53	(Krishnan et al.,

EC site	Ecosystem	Lat	Lon	Year	C balance[a] − modeled				C balance[a] − derived from EC measurements				
					GPP	Re	NEP	%▲[b]	GPP	Re	NEP	%▲[b]	Source[f]
	forest			2003[e]	2105	1890	215		2242	1985	256		2009)

a. Modeled and measured C balance units are in g C m^{-2} yr^{-1}.

b. The% of change in NEP of the drought year compared to non-drought year ((drought − non-drought)/non-drought) × 100).

c. Hydrological year: 23, October to 22, October of the next year (Ma et al., 2007).

d. Drought year.

e. Non-drought year (reference year).

f. EC dataset processed at ORNL, as part of the NACP Site-Level Synthesis.

At an hourly time scale, both modeled and EC CO_2 and energy fluxes were shown to be strongly affected by water stress during drought vs. non-drought years at the CA-Let site (Fig. 2). Both the measured and modeled hourly fluxes for selected summer days (days 178–188), under NARR weather, indicated greater declines in LE effluxes (Fig. 2c1) and CO_2 influxes (Fig. 2d1) in the drier year of 2001 than in the wetter 2002 (Fig. 2 (c2, d2)). Greater declines in CO_2 influxes than in effluxes were modeled in 2001 compared to 2002, causing sharp declines in NEP that changed the grassland from a sink to a source of carbon during drought. These greater declines were due in the model to soil drying, which forced greater midafternoon declines in $\psi_{c,}$ and g_c (Fig. 2b1) to balance U with E_c and consequently lower LE effluxes as described in Section 2.1. Lower g_c also induced a decline in rate of CO_2diffusion, hence lower CO_2 fixation in 2001 compared to 2002 (Fig. 2d1). These key modeled responses of net CO_2 exchange under contrasting weather in 2001 and 2002 were well captured at CA-Let. In 2001 modeled GPP and NEP declined by 73% and 95% respectively compared to 2002, resulting in a much smaller sink during the 2001 drought year (Table 2). These results indicate a realistic response of modeled GPP and NEP to interannual variability in precipitation (Section 2.4.1). The modeled result was corroborated by 69% and 94% declines in EC-derived annual GPP and NEP respectively in 2001 compared to 2002 (Table 2).

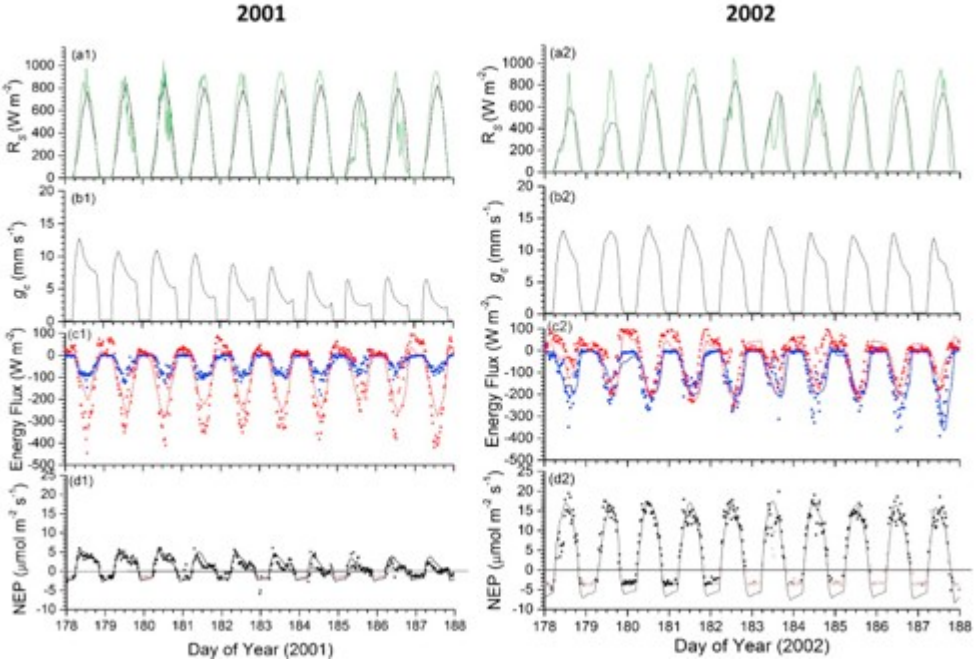

Fig. 2. Mixed grass prairie in Lethbridge (CA-Let): comparison of (a1, a2) hourly measured (green) and NARR (black) incoming short wave radiation (R_s), (b1, b2) canopy conductance (g_c), (c1, c2) latent (blue) and sensible (red) fluxes and (d1, d2) CO_2 fluxes modeled (lines), and measured by EC (closed symbols), or gap-filled from EC measurements (open symbols) for drought year 2001(a1–d1) vs. non-drought year 2002 (a2–d2); +ve = influx, −ve = efflux. Measured fluxes. (For interpretation of the references to colour in this figure legend, the reader is referred to the web version of this article.)

Source: (Flanagan and Adkinson, 2011)

Uncertainty associated with gridded model drivers such as NARR and UNASM could have affected the accuracy of the model in comparisons with site-level data. For instance, incoming shortwave radiation from NARR was underestimated in both 2001 and 2002 (Fig. 2(a1, a2)), resulting in lower H and LE than was measured (Fig. 2(c1, c2)). This underestimation of radiation was noted in a detailed analysis of uncertainties in the model estimates associated with model drivers (NARR and UNASM) for six EC sites in an earlier study (Mekonnen et al., 2016b) indicating that NEP modeled with these gridded inputs had less accurate diurnal and seasonal patterns than NEP modeled with inputs from site measurements for some sites, when tested against NEP derived from EC flux measurements.

3.1.2. Continental scale

The reductions in modeled annual GPP demonstrated at the EC sites (Table 2) were apparent at the continental scale, in which spatial patterns of reductions in modeled annual GPP were shown in regions affected by the 2002 drought across NA (Fig. 3a1). The spatial patterns indicated smaller modeled GPP in 2002 for most parts of the southwest and the Great Plains (excluding the Lethbridge region where the drought was ended in 2002 by rainfall), attributed to the drought compared to a normal year in 2005 (Fig. 3b) in which relatively higher annual GPP was modeled (Table 2). The spatial patterns of reductions in modeled GPP in the drought affected regions were corroborated by the similar patterns of reduced MODIS and EC-derived GPP in 2002 vs. 2005 (Fig. 3), with GWR for modeled vs. MODIS GPP (R^2 = 0.85 for 2002 and 0.86 for 2005) and modeled vs. EC-derived GPP (R^2 = 0.82 for 2002 and 0.80 for 2005). The reduction in GPP in 2002 vs. 2005 were modeled as much as ~500 g C m^{-2} yr^{-1}, particularly in the great plain regions and similar reductions were shown from MODIS and EC-derived GPP (Fig. 3 (c1, c2, c3)).

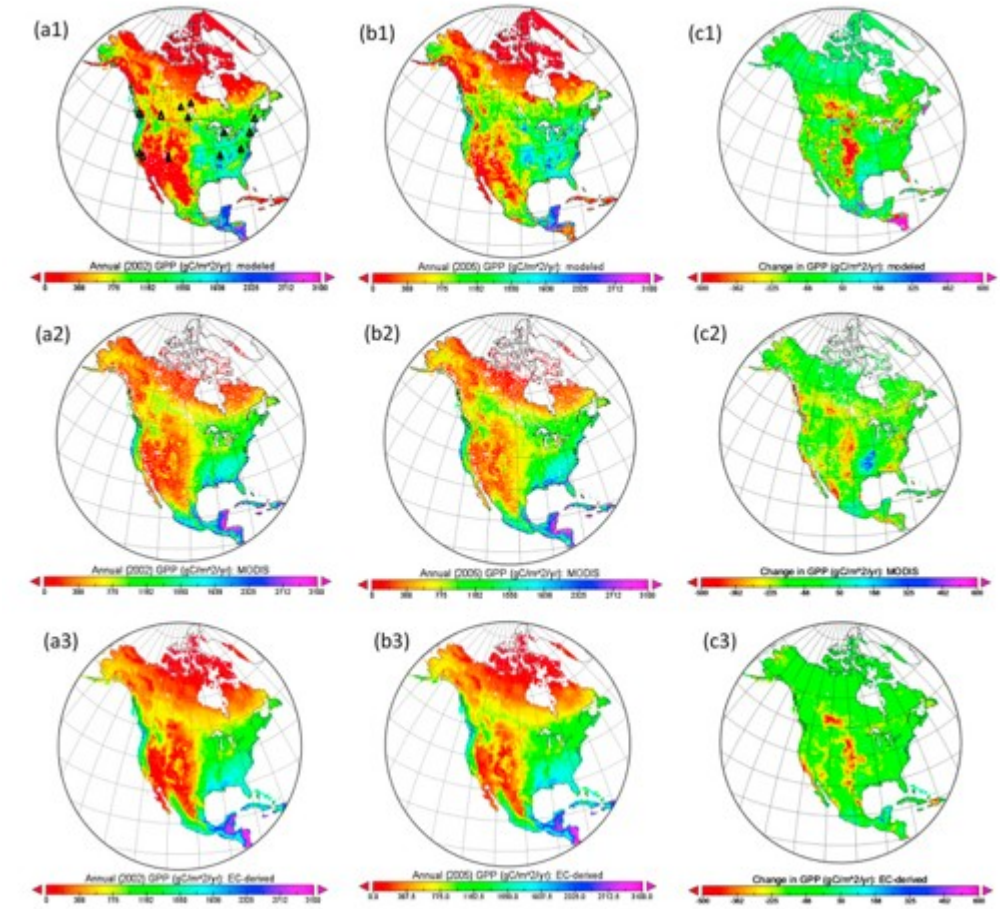

Fig. 3. Comparison of spatial patterns in modeled annual GPP (a1, b1), MODIS GPP (a2, b2) and GPP derived from network of EC towers (a3, b3) (Jung et al., 2011) for 2002 (drought) vs. 2005 (non-drought) years for North America modeled vs. MODIS GPP (R^2 = 0.85 for 2002 and 0.86 for 2005) and modeled vs. EC-derived GPP (R^2 = 0.82 for 2002 and 0.80 for 2005) and (c1, c2, c3) are changes in annual GPP (2002–2005). Black triangle symbols on (a1) are locations of EC sites in Table 2.

3.2. Major drought events and their impacts on productivity

3.2.1. Regional impacts on GPP and LAI

Spatial patterns of SPI for NA in June, July and August of 1988 and 2002 indicated declines of precipitation from long-term (1979–2010) monthly normals, well captured by NARR, in regions affected by two of the major drought events of NA in recent decades (Fig. 4). Growing season SPI values for most parts of the Great Plains and Midwest were extremely low (SPI < −2) indicating severely dry conditions in 1988 compared to the long-term normal (Fig. 4(a1, a2, a3)). Similarly, in 2002 SPI remained low (SPI < −2) for most parts of the southwest and the great plains, demonstrating a drought condition more pronounced in this region than in the rest of NA (Fig. 4(b1, b2, b3)).

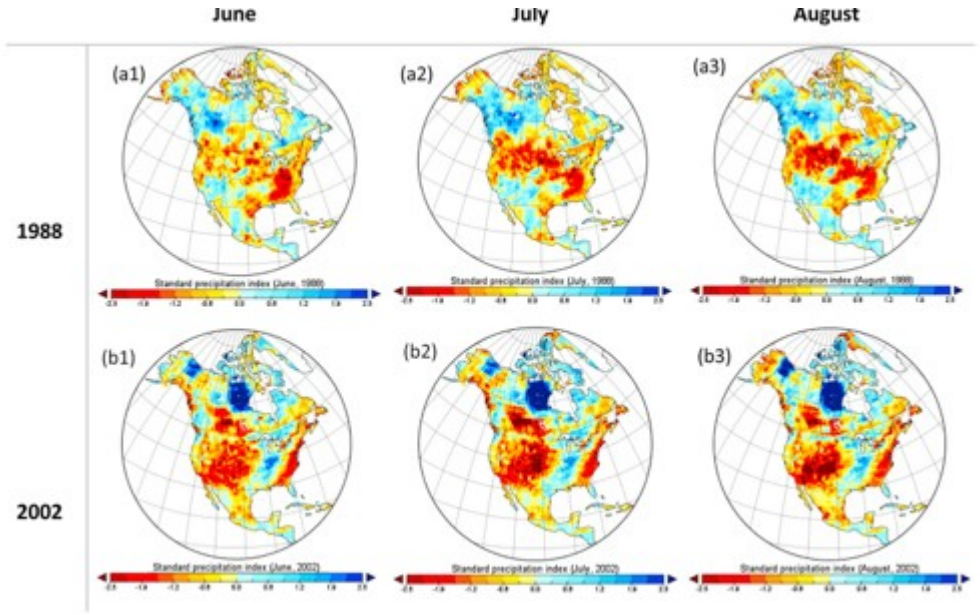

Fig. 4. Spatial patterns in standard precipitation index (SPI) for June, July and August during major drought events (1988 and 2002) of North America: NARR precipitation data range to calculate SPI 1979–2010.

The spatial patterns of declines in the growing season SPI (Fig. 4) had patterns similar to reductions in annual modeled GPP from the long-term normal in 1988 (Fig. 5a) and 2002 (Fig. 5b). Reductions in modeled mid-August LAI from the long-term mean, driven by lower GPP which reduced carbon allocation to foliage and hastened senescence, and by reduced Ψt which slowed leaf expansion, were shown in the drought-affected regions compared to regions that were not affected by the drought (Fig. 6(a1, a2)). The spatial patterns of these reductions in modeled LAI was corroborated by similar patterns of reductions in mid-August AVHRR NDVI of the corresponding years (Fig. 6a1 vs. 4-4b1; 4-4a2 vs. 4-4b2) resulting in a good agreement and close similarity in spatial patterns (GWR $R^2 = 0.84$ for 1988 and 0.71 for 2002), and demonstrating the skill of the model to capture drought effects on continental plant growth. In 1988 declines in LAI and NDVI were observed mainly in the southeast US and Great plains (Fig. 6(a1, b1)). Similar declines were observed in 2002 (Fig. 6(a2, b2)) in the west and southwest US, the Great Plains including parts of Alberta, Manitoba and Saskatchewan, consistent with the site-level declines in Table 2.

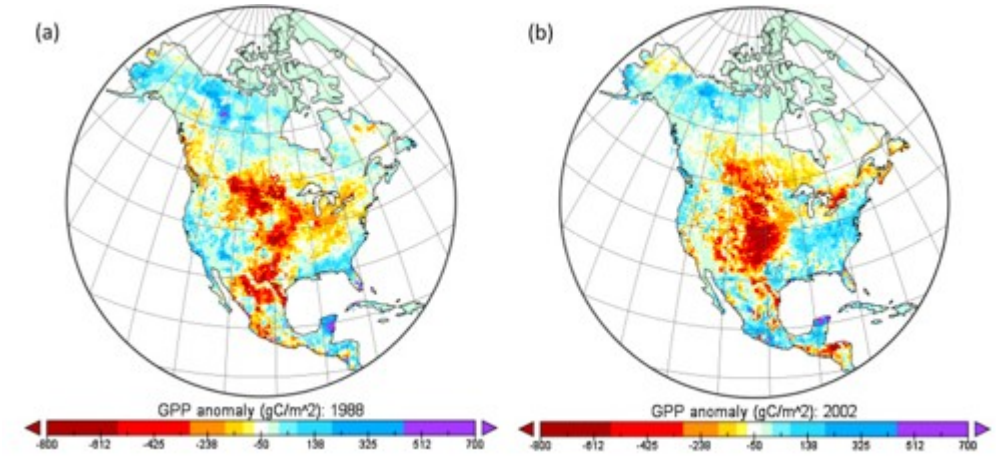

Fig. 5. Spatial changes in modeled annual GPP: values obtained by subtracting the long-term (1980–2010) annual average GPP from annual GPP during the drought years (1988, 2002).

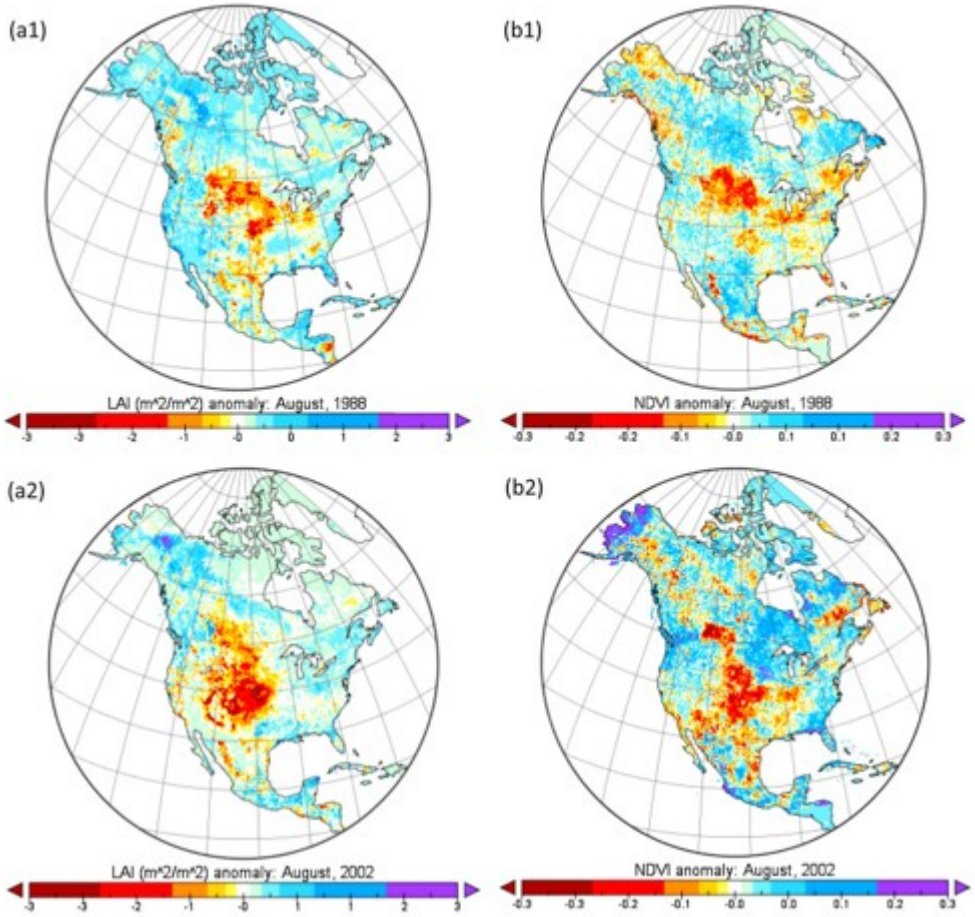

Fig. 6. Spatial anomalies in modeled mid-August LAI vs. AHVRR NDVI from their long-term means (equals zero) for the major drought years (1988, 2002) in North America: GWR R^2 = 0.84 for 1988 and 0.71 for 2002.

3.2.2. Continental impacts on NEP

The impacts of these major drought events on modeled carbon exchange at the continental scale were apparent from anomalies of spatially averaged GPP, net primary productivity(NPP), R_h and NEP from the long-term means with more negative values in 1988 and 2002 (Fig. 7(a1–d1)). The spatial average of the annual continental GPP in the model declined by 4.9% and 5.9% from the long-term mean in 1988 and 2002 respectively (Table 3). The drought in 1988 caused NPP to decline to 0.46 Pg C below the long-term annual average NPP (Fig. 7c1) for NA demonstrating a substantial loss in productivity. Similarly, the drought in 2002 caused annual NPP to decline to 0.63 Pg C below the long-term average. The decline in R_e was less than that in GPP (1.5% in 1988 and 2.7% in 2002), indicating that carbon fixation was more adversely affected by drought than was respiration. Consequently, NEP declined by 0.50 Pg C (92%) in 1988 and by 0.49 Pg C (90%) in 2002 from the long-term mean resulting in much smaller carbon sinks of +0.04 Pg C yr^{-1} and +0.05 Pg C yr^{-1} in 1988 and 2002 respectively (Table 3). These declines were similar to the modeled effects of drought on NEP at the site scale (Fig. 2; Table 2) and corroborated by EC-derived NEP as described in Section 3.1.1. Although significant effects of drought on the carbon balancewere apparent at continental scale, there were spatial variations in the carbon sources and sinks along a latitudinal gradient particularly in 2002, in which regions north of 45° N had greater declines in spatially averaged annual GPP (6.5%) than R_e (2.3%) resulting in a −0.02 Pg C yr^{-1} net source compared to parts of the continent south of 45° N with +0.074 Pg C yr^{-1} net carbon sink (Table 3). Overall, spatially averaged annual GPP and $R_e$declined in all the three spatial domains (NA, NA region north of 45° N and south of 45° N) during the drought years (Table 3).

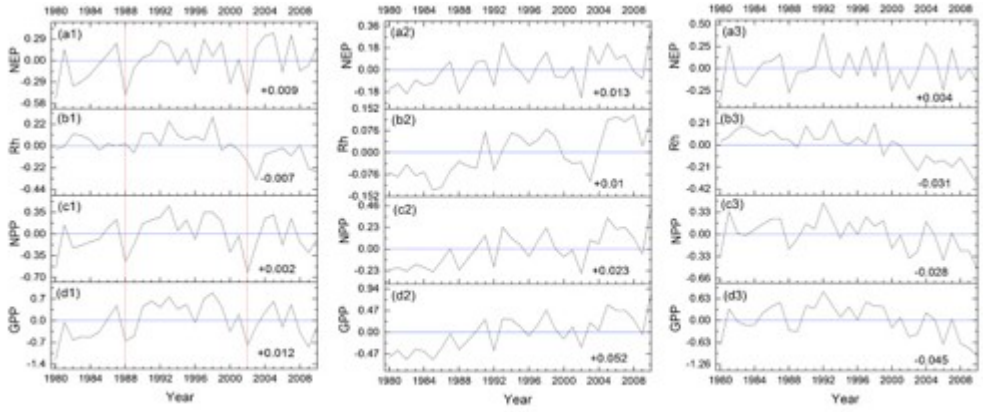

Fig. 7. Long-term anomalies and trends in spatially averaged GPP, NPP, R_h and NEP (Pg C yr^{-1}) from the long-term mean (equals zero) across different sub-regions of North America: (a1–d1) North America (a2–d2) above 45° N (a3–d3) below 45° N.

Table 3. Changes in spatially averaged ecosystem carbon fluxes for different sub-regions of North America modeled in 1988 and 2002.

Drought year	Flux component[a]	Annual total flux			Long-term annual average (1980–2010)			Flux change[e]			% Change[f]		
		NA[b]	>45 °N[c]	<45 °N[d]	NA	>45 °N	<45 °N	NA	>45 °N	<45 °N	NA	>45 °N	>45 °N
1988	GPP	13.74	5.14	8.60	14.45	5.54	8.91	−0.71	−0.40	−0.31	−4.9	−7.2	−3.5
	NPP	5.88	2.49	3.39	6.34	2.73	3.61	−0.46	−0.24	−0.22	−7.3	−8.8	−6.1
	R_e	13.70	5.12	8.57	13.91	5.32	8.59	−0.21	−0.20	−0.02	−1.5	−3.8	−0.2
	NEP	0.04	0.014	0.026	0.54	0.23	0.31	−0.50	−0.22	−0.28	−92.6	−93.9	−91.6
2002	GPP	13.60	5.18	8.41	14.45	5.54	8.91	−0.85	−0.36	−0.50	−5.9	−6.5	−5.6
	NPP	5.71	2.46	3.25	6.34	2.73	3.61	−0.63	−0.27	−0.36	−9.9	−9.9	−10.0
	R_e	13.54	5.20	8.34	13.91	5.32	8.59	−0.37	−0.12	−0.25	−2.7	−2.3	−2.9
	NEP	0.0	−0.0	0.07	0.5	0.23	0.31	−0.	−0.	−0.	−9	−10	−76

Drought year	Flux component[a]	Annual total flux			Long-term annual average (1980–2010)			Flux change[e]			% Change[f]		
		NA[b]	>45 °N[c]	<45 °N[d]	NA	>45 °N	<45 °N	NA	>45 °N	<45 °N	NA	>45 °N	>45 °N
		5[g]	2	4	4			49	25	24	0.7	8.7	.1

a. Annual total fluxes in Pg C yr^{-1}.

b. Spatial domain of terrestrial region of North America.

c. Spatial domain of terrestrial region of North America north of 45° N.

d. Spatial domain of terrestrial region of North America south of 45° N.

e. Changes in drought year flux from the long-term year (annual flux − long-term mean).

f. Percentage of change in drought year flux from the long-term mean ((annual flux − long-term mean)/long-term mean) × 100.

g. Equals CarbonTracker CT2013 B estimate for 2002 = +0.05 Pg C yr^{-1} and 2008 = +0.18 Pg C yr^{-1}(http://www.esrl.noaa.gov/gmd/ccgg/carbontracker, Accessed March, 10, 2015).

3.3. Interannual variability in precipitation and productivity 1980–2010

Much of the long-term interannual variability in modeled mid-August LAI was controlled by variations in climate variables, mainly precipitation as shown by similarities in spatial patterns of the RSD (Fig. 8(a, b)). The RSDs of LAI and precipitation were shown to vary spatially across the continent (Fig. 8(a, b)). Parts of the Great Plains, southwest US and northern Mexico were shown to have larger RSD for both modeled LAI and NARR precipitation, indicating that this sub-region of the continent had greater interannual variability in productivity controlled by the interannual variability in precipitation (Fig. 8a). This modeled result was corroborated by the higher interannual variability apparent in the mid-August NDVI from AVHRR (Fig. 8c). Spatially averaged SPI values for this sub-region of NA became increasingly negative from shorter time scales (1 month) to longer time scales (24 months) during 1988 and 2002, indicating longer, more severe drought conditions during those years (Fig. 9(a1–d1)). The impacts of these droughts were shown to cause a decline in spatially averaged productivity modeled during the drought years, shown by the lowest GPP, NPP and R_h over the last three decades (Fig. 9(b2, c2, d2)). Consequently, NEP values were lower than the long-term mean such that ecosystems in these regions lost more carbon during those drought years (Fig. 9a2).

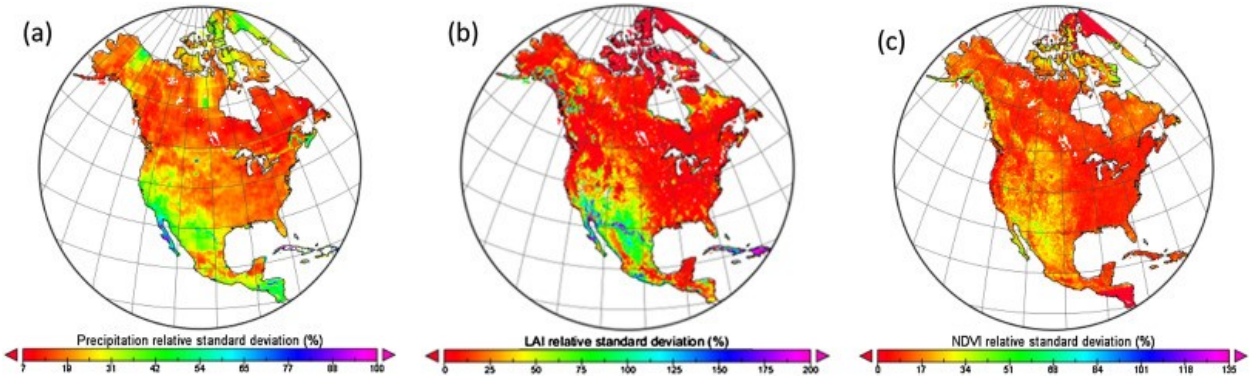

Fig. 8. Relative standard deviation (%) for long-term (1980–2010) annual (a) NARR precipitation, (b) modeled mid-August LAI and (c) mid-August NDVI (1982–2006).

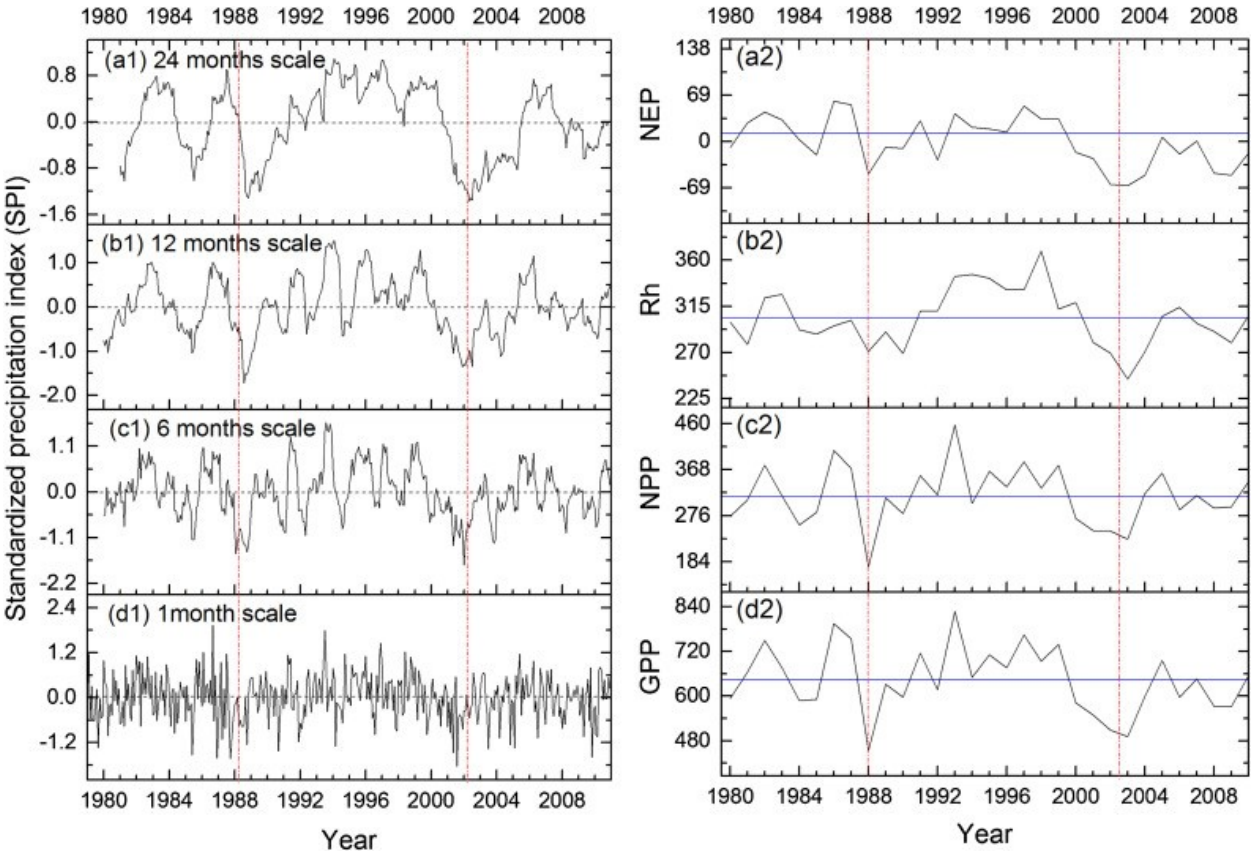

Fig. 9. (a1–d1) Standardized precipitation index (SPI) at different time scales (moving average for 3, 6, 12 and 24 months), and (a2–d2) spatial average annual fluxes (g C m^{-2} yr^{-1}) for the most drought affected sub-region of North America (Great Plains, southwest US and northern Mexico).

3.4. North American terrestrial carbon budget

3.4.1. Sources and sinks

Long-term annually averaged GPP, R_e and NEP in the model exhibited large spatial variability at the continental scale (Fig. 10). The southeast and Pacific northwest coasts, the Midwest and southern Mexico had higher average annual GPP and NEP (Fig. 10 (a, c)) and these regions were dominated by forests and croplands. The south and the southwest US and northern Mexico had lower modeled GPP and NEP due to less vegetation cover as a result of drier climates. Higher latitude regions had lower productivity as a result of cooler climates with shorter growing seasons. Modeled R_e (Fig. 10b) generally varied with GPP (Fig. 10a) because GPP drove biomass growth and hence R_a, and NPP drove litterfall and hence R_h.

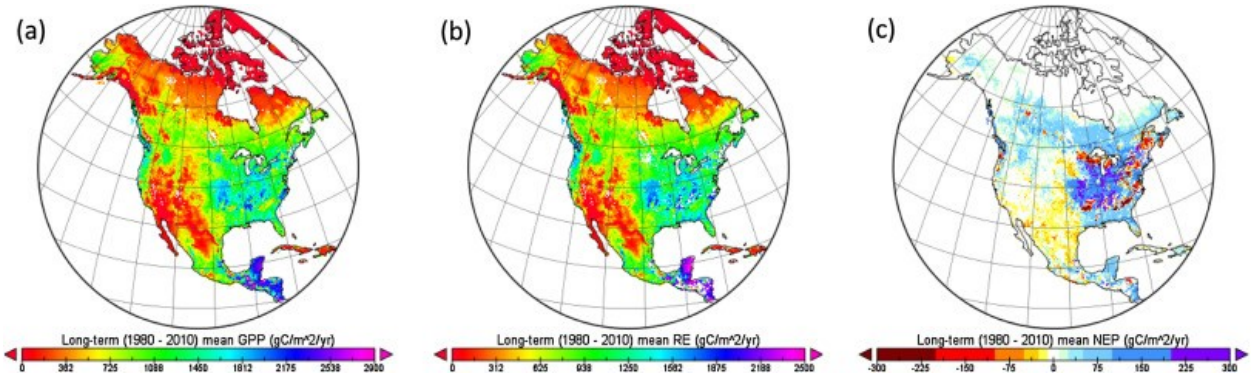

Fig. 10. Long-term (1980–2010) modeled mean annual (a) GPP, (b) RE and (c) NEP of North America: positive NEP implies sinks and negative NEP sources. Localized red spots in (c) indicate carbon sources caused by severe disturbance effects on NEP during the modeled period. (For interpretation of the references to colour in this figure legend, the reader is referred to the web version of this article.)

Regional differences in GPP vs. R_e caused most boreal, eastern temperate and Pacific northwest ecosystems to be modeled as carbon sinks, apparent in higher NEP, except for localized areas with recent fire which were modeled as carbon sources following the disturbances (Fig. 10c). Moreover, some parts of Mediterranean California, southwest US, northern Mexico and parts of western coastlines of Alaska were also modeled as carbon sources. Overall the entire NA continent was modeled as a carbon sink over the last three decades (Table 4). We estimated an average annual (2000–2005) GPP of 14.4 Pg C yr^{-1} for NA (Table 4). Ecosystem respiration was estimated 13.8 Pg C yr^{-1} resulting in 0.6 Pg C yr^{-1}NEP. The carbon emission as a result of fire disturbance resulted in net biome productivity (NBP = GPP − R_e − emission from disturbance) of 0.54 Pg C yr^{-1} (Table 4; Fig. 10c). Average annual (2000–2005) fossil fuel carbon emission of NA was 1.8 Pg C yr^{-1}, of which terrestrial NBP offset ~30%, resulting in net emission of 1.26 Pg C yr^{-1} (Table 4). This emission excluded the net amount of carbon taken up by water bodies within the spatial domain of NA landmass, which we have not accounted for, as our simulation domain was the terrestrial biosphere. However only 0.03% and 3.2% of fossil fuel emissions were offset by the terrestrial biosphere in 1988 and 2002 respectively, leaving almost all fossil fuel emissions in the atmosphere. Although the NA biosphere was modeled as a long-term sink, the significant drops in NBP during the drought years (1988 and 2002) offset 28% of the long-term carbon gains over the last three decades.

Table 4. Comparison of carbon budget estimates of different models for NA.

[b]Moderate Resolution Imaging Spectroradiometer MOD17 product:(Heinsch et al., 2006): http://modis.gsfc.nasa.gov/.

[c]CarbonTracker is a CO_2 measurement and modeling system: Net ecosystem exchange(NEE) = 0.65 Pg C yr^{-1} (Peters et al., 2007).

Estimates	Time	GPP	NPP	Ra	Rh	NEP	NBP	Net emission[g]
ecosys	2000–2005	14.4	6.3	8.1	5.7	0.6	0.54	1.26
NACP[a]	2000–2005	12.2–32.9			5.6–13.2	−0.7 to (+1.7)[h]		
MODIS[b]	2000–2005	13.4						
CarbonTracker[c]	2000–2005						0.65/0.44[i]	
EC-derived GPP[d]	2000–2005	14.8						
CO_2 Inversion[e]	2004						0.57	
SOCCR[f]	2003						0.51	1.35

[a]North American Carbon Program regional interim synthesis:(Huntzinger et al., 2012): mean NEP of +0.4 Pg C yr^{-1} for prognostic models and +0.9 Pg C yr^{-1} for diagnostic models

[b]Moderate Resolution Imaging Spectroradiometer MOD17 product:(Heinsch et al., 2006): http://modis.gsfc.nasa.gov/.

[c]CarbonTracker is a CO_2 measurement and modeling system: Net ecosystem exchange (NEE) = 0.65 Pg C yr^{-1}(Peters et al., 2007).

d. GPP derived and upscaled from network of EC observations (Jung et al., 2011).

e. Carbon flux inversion: (Schuh et al., 2010).

f. The first state of the carbon cycle report: (King et al., 2007).

g. Net emission (fossil fuel emission (1.8 Pg C (Boden et al., 2013)) − Net biome productivity (NBP)).

h. Mean NEP of +0.4 Pg C yr^{-1} for prognostic models and +0.9 Pg C yr^{-1} for diagnostic models.

i. CarbonTracker CT2013 B estimate = 0.44 Pg C yr^{-1} (http://www.esrl.noaa.gov/gmd/ccgg/carbontracker/).

3.4.2. Decadal trends in C exchange

Despite overall increases in long-term spatially averaged trends of NA modeled GPP (+0.12 Pg C $decade^{-1}$), NPP (+0.02 Pg C $decade^{-1}$) and NEP (+0.09 Pg C $decade^{-1}$) in recent decades (Fig. 7(a1–d1)), the impacts of the major droughts on these trends varied across regions. Although NEP dropped during droughts in 1988 and 2002 (Fig. 7a2), the northern ecosystems (north of 45° N) were stronger sinks with an average increase in NEP of +0.13 Pg C $decade^{-1}$ as a result of greater GPP (0.52 Pg C $decade^{-1}$) with longer growing

season (Fig. 7a2). In regions south of 45° N NEP increased by 0.04 Pg C decade^{-1}(Fig. 7a3), but this increase was mainly attributed to a relatively greater decline in R_e(-0.48 Pg C decade^{-1}) than in GPP (-0.45 Pg C decade^{-1}) (Fig. 7d3), as a result of greater increases in GPP than R_e in the eastern forests. The greater decline in GPP than R_e in the drought-affected southwest US resulted in increasing sources (Fig. 10c), indicating that projected increases in dryness (IPCC, 2013) in these parts of NA could enhance net carbon release and reduce net carbon sink of the continent.

4. Discussion

4.1. Major drought events and long-term trends in productivity

The soil-plant-atmosphere hydraulic scheme in *ecosys* described in Section 2.1, and demonstrated at CA-Let (Fig. 2) was shown to capture modeled drought effects at the site scale (Fig. 2) resulting in a grassland to change from a strong sink (modeled vs. EC-derived NEP = 204 vs. 295 g C m^{-2} yr^{-1}) in 2002 to a much smaller sink (modeled vs. EC-derived NEP = 10 vs. 18 g C m^{-2} yr^{-1}) during the 2001 drought (Table 2). A decline in LE (Eqs. B1b, c) relative to H (Eq. B1d) was also shown to be caused by one in g_c (Eq. B2) that forced commensurate declines in CO_2 fixation (Eq. C1).

At the continental scale, these processes were shown to reduce modeled GPP both in 1988 and 2002 which were mainly attributed to the water stress observed in NARR (SPI < −1) in the drought affected regions (Fig. 4). We also have modeled a concurrent reduction in R_e in both drought years (Fig. 7) which was caused by a reduction in the supply of labile carbon from a decline in GPP (van der Molen et al., 2011) and less moisture availability for microbial activity hence a decline in R_h (Eq. A11). However, a reduction in precipitation apparent from negative SPI in eastern forests of NA (Fig. 4) during 2002 was not shown to greatly decrease modeled GPP (Fig. 5) and LAI (Fig. 6), and this was corroborated with the NDVI(Fig. 6) and observed values from EC flux sites (e.g. US-Ha1, US-UMB, US-Ho1) (Table 2). These responses of eastern forests to lower SPI could be attributed to deep-rooted trees that sustained water availability and to excess precipitation relative to potential evapotranspiration.

Overall, the drought events increased net carbon releases to the atmosphere shown by the declines in modeled NEP (Table 3) and these were mainly attributed to the greater sensitivity to water stress of GPP than R_e. A study (Schwalm et al., 2010) using a global network of EC towers reported that GPP was 50% more sensitive to drought than was R_e across wide range of biomes. Therefore, a reduction in GPP could be larger than a reduction in R_e during drought, resulting in a decline in NEP and consequently changing ecosystems to net sources (Novick et al., 2004, van der Molen et al., 2011). Spatially averaged trends of modeled NEP for the drought affected sub-regions of NA (Fig. 9a2) indicated that the declines in NEP persisted after the drought years of 1988 and 2002, demonstrating carry-over effects to the next year of the drought events and indicating that drought can still affect the ecosystem

carbon dynamics after the initial declines in GPP and R_e. This effects were attributed in the model to drought-related depletion in reservoirs of soil moisture and plant carbohydrates (van der Molen et al., 2011) that were not completely replenished after the drought events (Grant et al., 2006a). Consequently, complete recovery of NEP to the pre-drought values could take up to 2 years (Fig. 9a2) or more, depending on drought intensity and duration, as found by Arnone et al. (2008).

Although the NA terrestrial biosphere was modeled to be a carbon sink over the last three decades (Table 3), the major drought events such as those in 1988 and 2002 (Fig. 7a1) adversely affected continental carbon exchange by reducing this sink and hence controlled much of the interannual variability. The drought-affected regions such as the southwest and the Great Plains and northern Mexico had high interannual variability of modeled mid-August LAI, NARR precipitation and NDVI (Fig. 8) that could be a result of frequent occurrences in El Niño–Southern Oscillation (ENSO). In an earlier study using *ecosys* (Fig. 12 of Mekonnen et al. (2016a)) smaller modeled GPP during the major droughts in 1988, 2001/02 and 2008/09 was associated with the cold phase of ENSO with large negative Multivariate ENSO Index (MEI) indicating that much of the interannual variability of NA GPP was controlled by ENSO events. Herweijer et al. (2007) reported that spatial variability of major droughts events reconstructed from networks of tree-ring chronologies were similar to ENSO patterns mainly in the southwest of US with an opposite effect on the Pacific Northwest. Similarly, Ropelewski and Halpert (1986) reported that patterns of NA precipitation departures from the long-term normal were associated with ENSO events for western and southeastern US and northern Mexico, suggesting that ENSO events could mainly control the major drought events in those regions. IPCC AR4 (2007) climate model projections have also shown that southwest US, similar to the subtropical dry zones of the world, will dry and expand to the north due to increasing warming (Cook et al., 2010) and this expansion could have a significant impact on the ecosystem productivity and carbon budget of NA.

4.2. Spatial and temporal patterns of NA carbon budget

The Great Plains, northern, eastern and southeastern regions of NA have mainly been carbon sinks over the last three decades, except where stand-replacing disturbances occurred (Fig. 10c). These effects of disturbances on NEP are explicitly modeled in *ecosys*and tested against EC measurements as described in Grant et al. (2010) and Wang et al. (2011). Regions dominated by forests and croplands were stronger sinks compared to non-forested regions, whereas drier regions such as the southwest were mainly carbon sources (Fig. 10c). This modeled result was consistent with some of the results reported in the North America Carbon Program (NACP) regional interim synthesis model intercomparison (Huntzinger et al., 2012) in which the Midwest and southeast US were simulated as carbon sinks by some models. Boreal regions of NA were mainly sinks for most of the models in this intercomparison, as modeled here (Fig. 10c). Our result indicated that on an

annual scale central and northern Mexico were net carbon sources which was consistent with some other studies (Cairns et al., 2000, Pacala et al., 2007) that reported Mexico as a net carbon source. This source was partly attributed to land use changes as a result of the ongoing deforestation in Mexico reported in Cairns et al. (2000) and Pacala et al. (2007). Our model results for the spatial distributions of the carbon sinks were also consistent with another report (Peters et al., 2007) that estimated sinks mainly in the deciduous forests and the east coast. Xiao et al. (2011) calculated sources and sinks of conterminous US by integrating NEE estimates of EC towers and MODIS products, and found that most of the sinks were dominated by evergreen and deciduous forests and savannas.

Previous studies that used several approaches to estimate land-atmosphere carbon exchange across NA have presented wide ranges of annual estimates of ecosystem productivity. Huntzinger et al. (2012) estimated average annual (2000 − 2005) NEP for 19 terrestrial biospheric models, with averages of +0.4 Pg C yr^{-1} for prognostic models and +0.9 Pg C yr^{-1} for diagnostic models. Our NEP estimate of +0.6 Pg C yr^{-1} was close to the average of the prognostic and diagnostic models (Table 4). Our continental modeled NBP of +0.54 Pg C yr^{-1} was close to an estimate of +0.505 Pg C yr^{-1} from the first North American State of the Carbon Cycle Report by King et al. (2007) for 2003, which was computed based on wide range of carbon inventories. Our NBP was also close to one of +0.57 Pg C yr^{-1} from a study (Schuh et al., 2010) in which top-down atmospheric inversion modeling method was used to estimate carbon sources and sinks from atmospheric CO_2 concentrations and atmospheric transport in 2004. In another study using CarbonTracker, Peters et al. (2007)estimated an annual average (2000–2005) carbon sink of +0.65 Pg C yr^{-1}, however the latest estimates of CarbonTracker CT2013 B resulted in net carbon sink of +0.44 Pg C yr^{-1}(Table 4). The smaller modeled carbon sink in 2002 (+0.05 Pg C yr^{-1} in Table 3 and Fig. 11) was consistent with a similar estimate of +0.05 Pg C yr^{-1} from CarbonTracker CT2013B, an estimated decline of 88% (0.37 Pg C yr^{-1}) from the long-term (2000–2010) mean (0.42 Pg C yr^{-1}). A 31% (0.17 Pg C yr^{-1}) decline in modeled NEP from the long-term mean during the drought in 2008 (Fig. 7a; Fig. 11) was also consistent with a 43% (0.18 Pg C yr^{-1}) decline in carbon sink estimated from Carbon Tracker in 2008. In a more recent study, King et al. (2015) summarized estimates from atmospheric inversion, inventory-based and TBMs and stated that NA was a carbon sink with annual average for 2000–2009 ranging from 0.27 Pg C yr^{-1} to 0.89 Pg C yr^{-1}, and with the mean +0.47 Pg C yr^{-1}, a range similar to that modeled here (Fig. 11). These NEP in the model were driven by an average GPP of 14.44 Pg C yr^{-1}, similar to one of 14.8 Pg C yr^{-1} from EC-derived GPP and 13.4 Pg C $yr^{-1}$from the MODIS MOD17 product (2000 − 2005) (Table 4).

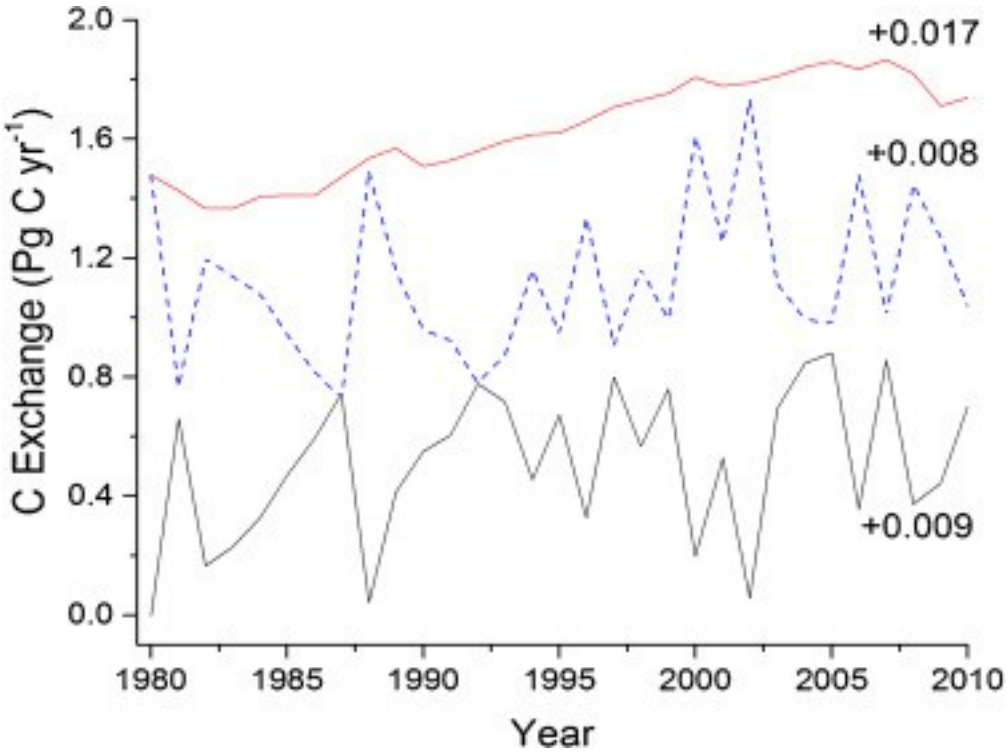

Fig. 11. Long-term trends in modeled annual NEP (Black line), annual anthropogenic fossil fuel emissions (red line) and net carbon emissions (annual NEP subtracted from the annual fossil fuel emission) without considering the carbon that could be sequestered in water bodies in North America (blue line): North America fossil fuel emission data was obtained from Boden et al. (2013). (For interpretation of the references to colour in this figure legend, the reader is referred to the web version of this article.)

Although NA terrestrial ecosystems are estimated collectively to be a net carbon sink, fossil fuel emissions are a much greater source of carbon to the atmosphere. Fossil fuel emissions in NA have been increasing at a rate of 0.017 Pg C yr^{-1} which is greater than that of the modeled terrestrial sink in NA over the last three decades (0.009 Pg C yr^{-1}) (Fig. 11). This greater rate causes a net increase of 0.008 Pg C yr^{-1} in net emissions without considering the carbon that could be taken up by the water bodies within the NA spatial domain. On an annual basis, only about half of the emission from fossil fuel and land cover change resides in the atmosphere and the rest is taken up by the oceans and terrestrial biospheres (Baker et al., 2006, IPCC, 2007). Our modeling result indicated that on average 30% of the total fossil fuel emission was taken up by the terrestrial biosphere of NA in 2000–2005 (0.54/1.8 Pg C yr^{-1} in Table 4). This result agreed with King et al. (2007) who estimated that 30% of the NA fossil fuel emission was offset by sinks of the terrestrial biosphere in 2003.

Although stronger carbon sinks were modeled with recent warming in northern ecosystems as a result of greater GPP (Fig. 7) with longer growing season, projected increases in frequency and intensity of drought under future climate change scenarios could enhance carbon release hence may reduce net carbon sink of the continent. The adverse impacts of water stress

shown by the significant declines in the continental carbon sink during the major drought events may further be amplified by projected warming in most parts of NA. Thus, on annual time scale long-term carbon sinks of NA may not be sustained indefinitely under future climates. The impacts of future climate change on these sinks will be examined with *ecosys* in future studies. In this regard, the extent to which climate extremes affect regional to global carbon cycle need to be carefully examined and better understanding of ecosystem processes that control drought is crucial to predict future impacts and process based ecosystem models can be coupled with climate models to develop early warning systems of drought occurrences.

Acknowledgements

Funding was provided by NSERC Discovery Frontiers (DF) grant through Arctic Development and Adaptation to Permafrost in Transition (ADAPT). We acknowledge the Multi-scale Synthesis and Terrestrial Model Intercomparison Project (MsTMIP; http://nacp.ornl.gov/MsTMIP.shtml) for providing support in environmental driver data. Funding for MsTMIP activity was provided through NASA ROSES Grant #NNX10AG01A. Data management support for preparing, documenting, and distributing model driver and output data was performed by the Modeling and Synthesis Thematic Data Center at Oak Ridge National Laboratory (ORNL; http://nacp.ornl.gov), with funding through NASA ROSES Grant #NNH10AN681. EC flux data was obtained from NACP North American Carbon Program (NACP) Site-Level Synthesis dataset. Data products in this study are archived at the ORNL DAAC (http://daac.ornl.gov). Computational facility for *ecosys* was provided by WestGrid supercomputing infrastructure (https://www.westgrid.ca).

References

W.M. AlleyThe Palmer drought severity index: limitations and assumptions J. Climate Appl. Meteorol., 23 (7) (1984), pp. 1100-1109

J.A. Arnone III, *et al.*Prolonged suppression of ecosystem carbon dioxide uptake after an anomalously warm year Nature, 455 (7211) (2008), pp. 383-386

D.F. Baker, *et al.*TransCom 3 inversion intercomparison: impact of transport model errors on the interannual variability of regional CO 2fluxes, 1988–2003 Global Biogeochem. Cycles, 20 (1) (2006), pp. n/a-n/a

D. Baldocchi, *et al.*FLUXNET: A new tool to study the temporal and spatial variability of ecosystem-scale carbon dioxide, water vapor, and energy flux densities Bull. Am. Meteorol. Soc., 82 (11) (2001), pp. 2415-2434

Barr, A.G. et al. 2013. NACP Site: Tower Meteorology, Flux Observations with Uncertainty, and Ancillary Data. ORNL Distributed Active Archive Center. 10.3334/ORNL DAAC/1178.

T.A. Boden, G. Marland, R.J. AndresGlobal, Regional, and National Fossil-Fuel CO2 Emissions Carbon Dioxide Information Analysis Center, Oak Ridge National Laboratory, U.S. Department of Energy, Oak Ridge, Tenn., U.S.A (2013), 10.3334/CDIAC/00001_V2013

E.O. Box, B.N. Holben, V. KalbAccuracy of the AVHRR vegetation index as a predictor of biomass, primary productivity and net CO2 flux Vegetatio, 80 (2) (1989), pp. 71-89

G. Caccamo, L. Chisholm, R.A. Bradstock, M. PuotinenAssessing the sensitivity of MODIS to monitor drought in high biomass ecosystems Remote Sens. Environ., 115 (10) (2011), pp. 2626-2639

M.A. Cairns, P.K. Haggerty, R. Alvarez, B.H. De Jong, I. OlmstedTropical Mexico's recent land-use change: A region's contribution to the global carbon cycle Ecol. Appl., 10 (5) (2000), pp. 1426-1441

T.N. Carlson, D.A. RipleyOn the relation between NDVI, fractional vegetation cover, and leaf area index Remote Sens. Environ., 62 (3) (1997), pp. 241-252

P. Ciais, *et al.*Europe-wide reduction in primary productivity caused by the heat and drought in 2003 Nature, 437 (7058) (2005), pp. 529-533

E.R. Cook, *et al.*Megadroughts in North America: placing IPCC projections of hydroclimatic change in a long-term palaeoclimate context J. Quaternary Sci., 25 (1) (2010), pp. 48-61

A. Dai, K.E. Trenberth, T. QianA global dataset of Palmer Drought Severity Index for 1870–2002: relationship with soil moisture and effects of surface warming J. Hydrometeorol., 5 (6) (2004)

Dentener, F., 2006. Global maps of atmospheric nitrogen deposition, 1860, 1993, and 2050. Data set. Available on-line (http://daac.ornl.gov) from Oak Ridge National Laboratory Distributed Active Archive Center, Oak Ridge, TN, USA.

L.B. Flanagan, A.C. AdkinsonInteracting controls on productivity in a northern Great Plains grassland and implications for response to ENSO events Global Change Biol., 17 (11) (2011), pp. 3293-3311

D. Gaumont-Guay, *et al.*Influence of temperature and drought on seasonal and interannual variations of soil, bole and ecosystem respiration in a boreal aspen stand Agric. For. Meteorol., 140 (1–4) (2006), pp. 203-219

C. Gough, C. Vogel, H. Schmid, H.-B. Su, P. CurtisMulti-year convergence of biometric and meteorological estimates of forest carbon storage Agric. For. Meteorol., 148 (2) (2008), pp. 158-170

M.L. Goulden, J.W. Munger, S.-M. Fan, B.C. Daube, S.C. WofsyExchange of carbon dioxide by a deciduous forest: response to interannual climate variability Science (1996)

M.L. Goulden, *et al.*An eddy covariance mesonet to measure the effect of forest age on land-atmosphere exchange Global Change Biol., 12 (11) (2006), pp. 2146-2162

R.F. Grant, L.B. FlanaganModeling stomatal and nonstomatal effects of water deficits on C fixation in a semiarid grassland J. Geophys. Res.-Biogeo., 112 (G3) (2007), p. G03011

R. Grant, *et al.*Crop water relations under different CO2 and irrigation: testing of ecosys with the free air CO2 enrichment (FACE) experiment Agric. Forest Meteorol., 95 (1) (1999), pp. 27-51

R.F. Grant, *et al.*Net ecosystem productivity of boreal aspen forests under drought and climate change: mathematical modelling with Ecosys Agric. For. Meteorol., 140 (1–4) (2006), pp. 152-170

R.F. Grant, *et al.*Intercomparison of techniques to model water stress effects on CO2 and energy exchange in temperate and boreal deciduous forests Ecol. Modell., 196 (3–4) (2006), pp. 289-312

R. Grant, T. Black, E. Humphreys, K. MorgensternChanges in net ecosystem productivity with forest age following clearcutting of a coastal Douglas-fir forest: testing a mathematical model with eddy covariance measurements along a forest chronosequence Tree Physiol., 27 (1) (2007), pp. 115-131

R.F. Grant, *et al.*Net biome productivity of irrigated and rainfed maize–soybean rotations: modeling vs. measurements Agron. J., 99 (6) (2007), p. 1404

R.F. Grant, *et al.*Interannual variation in net ecosystem productivity of Canadian forests as affected by regional weather patterns—a Fluxnet-Canada synthesis Agric. For. Meteorol., 149 (11) (2009), pp. 2022-2039

R. Grant, *et al.*Net ecosystem productivity of temperate and boreal forests after clearcutting—a Fluxnet-Canada measurement and modelling synthesis Tellus B, 62 (5) (2010), pp. 475-496

R. Grant, *et al.*Controlled warming effects on wheat growth and yield: field measurements and modeling Agron. J., 103 (6) (2011), pp. 1742-1754

R.F. Grant, E.R. Humphreys, P.M. Lafleur, D.D. DimitrovEcological controls on net ecosystem productivity of a mesic arctic tundra under current and future climates J. Geophys. Res., 116 (G1) (2011)

R.F. Grant, D.D. Baldocchi, S. MaEcological controls on net ecosystem productivity of a seasonally dry annual grassland under current and future climates: modelling with ecosys Agric. For. Meteorol., 152 (2012), pp. 189-200

R. GrantA review of the Canadian ecosystem model ecosys Modeling Carbon and Nitrogen Dynamics for Soil Management, CRC Press, Boca Raton, FL (2001), pp. 173-264

R.F. GrantNitrogen mineralization drives the response of forest productivity to soil warming: modelling in ecosys vs. measurements from the Harvard soil heating experiment Ecol. Model., 288 (2014), pp. 38-46

Y. Gu, *et al.*Evaluation of MODIS NDVI and NDWI for vegetation drought monitoring using Oklahoma Mesonet soil moisture data Geophys. Res. Lett., 35 (22) (2008)

M.J. Hayes, M.D. Svoboda, D.A. Wilhite, O.V. VanyarkhoMonitoring the 1996 drought using the standardized precipitation index Bull. Am. Meteorol. Soc., 80 (3) (1999), pp. 429-438

Heinsch, F., Reeves, M. and Votava, P., 2006. others 2003 User's Guide: GPP and NPP (MOD17A2/A3) Products NASA MODIS Land Algorithm Version 20, December 2, 2003. University of Montana.

I.M. Held, B.J. SodenWater vapor feedback and global warming Annu. Rev. Energy Environ., 25 (1) (2000), pp. 441-475

C. Herweijer, R. Seager, E.R. Cook, J. Emile-GeayNorth American droughts of the last millennium from a gridded network of tree-ring data J. Climate, 20 (7) (2007), pp. 1353-1376

T.G. HuntingtonEvidence for intensification of the global water cycle: review and synthesis J. Hydrol., 319 (1) (2006), pp. 83-95

D.N. Huntzinger, *et al.*North american carbon program (NACP) regional interim synthesis: terrestrial biospheric model intercomparison Ecol. Model., 232 (0) (2012), pp. 144-157

D. Huntzinger, *et al.*The North American Carbon Program multi-scale synthesis and terrestrial model intercomparison project—Part 1: overview and experimental design Geoscientific Model Dev., 6 (6) (2013), pp. 2121-2133

G.C. Hurtt, *et al.*The underpinnings of land-use history: three centuries of global gridded land-use transitions, wood-harvest activity, and resulting secondary lands Global Change Biol., 12 (7) (2006), pp. 1208-1229

IPCC, 2007. Climate Change 2007: The Physical Science Basis. Contribution of Working Group I to the Fourth Assessment Report of the Intergovernmental Panel on Climate Change [Solomon, S., D. Qin, M., Manning, Z., Chen, M., Marquis, K.B., Averyt, M.Tignor and H.L. Miller (eds.)]. Cambridge University Press Cambridge, United Kingdom and New York, NY, USA.

IPCC, 2013. Climate change 2013: The Physical Science Basis. Contribution of Working Group I to the fifth assessment report of the Intergovernmental Panel on Climate Change [Stocker TF, Qin D, Plattner G-K, Tignor M, Allen SK, Boschung J, Nauels A, Xia Y, Bex V, Midgley PM, eds]. Cambridge, UK & New York, NY, USA: Cambridge University Press.

P. Jamieson, R. Martin, G. Francis, D. WilsonDrought effects on biomass production and radiation-use efficiency in barley Field Crops Res., 43 (2) (1995), pp. 77-86

A. Jentsch, J. Kreyling, C. BeierkuhnleinA new generation of climate-change experiments: events, not trends Front. Ecol. Environ., 5 (7) (2007), pp. 365-374

M. Jung, K. Henkel, M. Herold, G. ChurkinaExploiting synergies of global land cover products for carbon cycle modeling Remote Sens. Environ., 101 (4) (2006), pp. 534-553

M. Jung, *et al.*Global patterns of land-atmosphere fluxes of carbon dioxide, latent heat, and sensible heat derived from eddy covariance, satellite, and meteorological observations J. Geophys. Res. (2011) (116(G3)

A. Karnieli, *et al.*Use of NDVI and land surface temperature for drought assessment: merits and limitations J. Climate, 23 (3) (2010), pp. 618-633

King, A.W. et al. 2007. The first state of the carbon cycle report (SOCCR): The North American carbon budget and implications for the global carbon cycle. The first state of the carbon cycle report (SOCCR): The North American carbon budget and implications for the global carbon cycle.

A. King, *et al.*North America's net terrestrial CO 2 exchange with the atmosphere 1990–2009

Biogeosciences, 12 (2) (2015), pp. 399-414

N. Kljun, *et al.*Response of net ecosystem productivity of three boreal forest stands to drought Ecosystems, 9 (7) (2006), pp. 1128-1144

W. Knorr, M. HeimannImpact of drought stress and other factors on seasonal land biosphere CO2 exchange studied through an atmospheric tracer transport model Tellus B, 47 (4) (1995), pp. 471-489

P. Krishnan, T.A. Black, R.S. Jassal, B. Chen, Z. NesicInterannual variability of the carbon balance of three different-aged Douglas-fir stands in the Pacific Northwest J. Geophys. Res. (2005–2012), 114 (G4) (2009)

T. Li, R.F. Grant, L.B. FlanaganClimate impact on net ecosystem productivity of a semi-arid natural grassland: modeling and measurement Agric. For. Meteorol., 126 (1) (2004), pp. 99-116

ArticleDownload PDFView Record in Scopus

A. Lindroth, *et al.*Storms can cause Europe-wide reduction in forest carbon sink Global Change Biol., 15 (2) (2009), pp. 346-355

S. Liu, *et al.*The unified North American soil map and its implication on the soil organic carbon stock in North America Biogeosciences, 10 (5) (2013), pp. 2915-2930

S. Ma, D.D. Baldocchi, L. Xu, T. HehnInter-annual variability in carbon dioxide exchange of an oak/grass savanna and open grassland in California Agric. For. Meteorol., 147 (3) (2007), pp. 157-171

T.B. McKee, N.J. Doesken, J. KleistThe relationship of drought frequency and duration to time scales Proceedings of the 8th Conference on Applied Climatology American Meteorological Society, Boston, MA(1993), pp. 179-183

Z.A. Mekonnen, R.F. Grant, C. SchwalmContrasting changes in gross primary productivity of different regions of North America as affected by warming in recent decades Agric. For. Meteorol., 218–219 (2016), pp. 50-64

Z.A. Mekonnen, R.F. Grant, C. SchwalmSensitivity of modeled NEP to climate forcing and soil at site and regional scales: implications for upscaling ecosystem models Ecol. Model., 320 (2016), pp. 241-257

F. Mesinger, *et al.*North American regional reanalysis Preprints AMS 2004 Annual Meeting, Seattle, WA (2004)

R.K. Monson, *et al.*Climatic influences on net ecosystem CO2 exchange during the transition from wintertime carbon source to springtime carbon sink in a high-elevation, subalpine forest Oecologia, 146 (1) (2005), pp. 130-147

R. Myneni, *et al.*Global products of vegetation leaf area and fraction absorbed PAR from year one of MODIS data Remote Sens. Environ., 83 (1) (2002), pp. 214-231

K. Novick, *et al.*Carbon dioxide and water vapor exchange in a warm temperate grassland Oecologia, 138 (2) (2004), pp. 259-274

R. Oren, *et al.*Estimating the uncertainty in annual net ecosystem carbon exchange: spatial variation in turbulent fluxes and sampling errors in eddy-covariance measurements Global Change Biol., 12 (5) (2006), pp. 883-896

Pacala, S. et al. 2007. The North American carbon budget past and present.

Y. Pan, *et al.*Age structure and disturbance legacy of North American forests Biogeosciences, 8 (3) (2011), pp. 715-732

J.S. Pereira, *et al.*Net ecosystem carbon exchange in three contrasting Mediterranean ecosystems—the effect of drought Biogeosciences, 4 (5) (2007), pp. 791-802

W. Peters, *et al.*An atmospheric perspective on North American carbon dioxide exchange: CarbonTracker Proc. Natl. Acad. Sci., 104 (48) (2007), pp. 18925-18930

M. Reichstein, *et al.*Modeling temporal and large-scale spatial variability of soil respiration from soil water availability, temperature and vegetation productivity indices Global Biogeochem. Cycles, 17 (4) (2003)

M. Reichstein, *et al.*Climate extremes and the carbon cycle Nature, 500 (7462) (2013), pp. 287-295

A.D. Richardson, *et al.*Influence of spring phenology on seasonal and annual carbon balance in two contrasting New England forests Tree Physiol., 29 (3) (2009), pp. 321-331

C.F. Ropelewski, M.S. HalpertNorth American precipitation and temperature patterns associated with the El Niño/Southern Oscillation (ENSO) Mon. Weather Rev., 114 (12) (1986), pp. 2352-2362

H.P. Schmid, C.S.B. Grimmond, F. Cropley, B. Offerle, H.-B. SuMeasurements of CO 2 and energy fluxes over a mixed hardwood forest in the mid-western United States Agric. For. Meteorol., 103 (4) (2000), pp. 357-374

A.E. Schuh, *et al.*A regional high-resolution carbon flux inversion of North America for 2004 Biogeosciences, 7 (5) (2010), pp. 1625-1644

C.R. Schwalm, *et al.*Assimilation exceeds respiration sensitivity to drought: a FLUXNET synthesis Global Change Biol., 16 (2) (2010), pp. 657-670

G.R. Shaver, *et al.*Global warming and terrestrial ecosystems: a conceptual framework for analysis BioScience, 50 (10) (2000), pp. 871-882

S. Urbanski, *et al.*Factors controlling C exchange on timescales from hourly to decadal at Harvard Forest J. Geophys. Res. (2005–2012), 112 (G2) (2007)

Z. Wan, P. Wang, X. LiUsing MODIS land surface temperature and normalized difference vegetation index products for monitoring drought in the southern Great Plains, USA Int. J. Remote Sens., 25 (1) (2004), pp. 61-72

Z. Wang, *et al.*Evaluating weather effects on interannual variation in net ecosystem productivity of a coastal temperate forest landscape: a model intercomparison Ecol. Model., 222 (17) (2011), pp. 3236-3249

Y. Wei, *et al.*The north american carbon program multi-scale synthesis and terrestrial model intercomparison Project—Part 2: environmental driver data Geoscientific Model Dev., 7 (6) (2014), pp. 2875-2893

J. Xiao, *et al.*Assessing net ecosystem carbon exchange of U. S: terrestrial ecosystems by integrating eddy covariance flux measurements and satellite observations Agric. For. Meteorol., 151 (1) (2011), pp. 60-69

M. Zhao, S.W. RunningDrought-induced reduction in global terrestrial net primary production from 2000 through 2009 Science, 329 (5994) (2010), pp. 940-943

J. Zscheischler, *et al.*Impact of large-scale climate extremes on biospheric carbon fluxes: an intercomparison based on MsTMIP data Global Biogeochem. Cycles, 28 (6) (2014), pp. 585-600

J.A. van Aardenne, F.J. Dentener, J.G.J. Olivier, C.G.M.K. Goldewijk, J. LelieveldA 1° × 1° resolution data set of historical anthropogenic trace gas

emissions for the period 1890–1990 Global Biogeochem. Cycles, 15 (4) (2001), pp. 909-928

M.K. van der Molen, *et al.*Drought and ecosystem carbon cycling Agric. For. Meteorol., 151 (7) (2011), pp. 765-773